Materials Science and Engineering B 318 (2025) 118259

Contents lists available at ScienceDirect

Materials Science & Engineering B

journal homepage: www.elsevier.com/locate/mseb

Advancing direct ethanol metal supported fuel cells with catalytic layer☆

S.G.M. Carvalho [a], F.N. Tabuti [a], E.I. Santiago [a], R. Abe [b], R.M. Guimarães [b], Y. Miura [c], Y. Fukuyama [c], F.C. Fonseca [a,*]

[a] Nuclear and Energy Research Institute, IPEN-CNEN/SP, São Paulo, SP, Brazil
[b] Nissan do Brasil Automóveis Ltda, R&D Departament, Rio de Janeiro, Brazil
[c] Nissan Motors Company, Ltd, Nissan Research Center, EV System Laboratory, Yokosuka-shi, Kanagawa, Japan

A B S T R A C T

Fuel cells are efficient power sources to play a role in the urgent energy transition. Direct ethanol fuel cells may boost the application of solid oxide fuel cell because ethanol is an efficient, sustainable, and readily available fuel. Metal supported solid oxide fuel cells provide the necessary mechanical properties to allow complex applications such as vehicles. Thus, the combination of a renewable fuel and a robust fuel cell may be a perfect combination for widespread decarbonization of transportation, facilitated by an economic viable and energetic efficient liquid fuel. However, several challenges remain to prolong the durability of such devices running on ethanol. We report on the significant improvement of the metal supported fuel cell stability operating at relatively low temperature (700 °C) with ethanol by adding a porous active catalytic layer with controlled microstructure using processing parameters compatible with the metal-supported solid oxide fuel cell technology.

1. Introduction

Fuel cells are efficient power sources to play a relevant role in the urgent energy transition. Such electrochemical devices are not limited to the Carnot cycle and directly convert the chemical energy of a fuel into electricity [1,2]. Moreover, both the modularity and reversibility of such electrochemical reactors allow for the combination of power-to-X technologies and energy conversion in a single device that can be designed in a large range of power for different applications [3–6]. Among various fuel cell technologies, the solid oxide fuel cells (SOFC's) distinguish themselves due to high operating temperatures (usually, in the 1000 °C – 600 °C range), which allows for wide selection of fuels and earth-abundant components. The main challenge for widespread adoption of such ceramic fuel cells lies in increasing their durability and decreasing cost. Traditionally, the SOFC's are ascribed to multi-kW stationary applications, but recent developments are expanding the applicability domains of this technology.

Metal-supported solid oxide fuel cells (M−SOFC) have emerged as an efficient advancement of the state-of-the-art anode-supported SOFC. Such devices fully explore the solid-state characteristics of SOFC's allowing for innovative designs and fabrication methods including different deposition technologies, various supports, and geometries comprising miniaturization and thin films, for instance [7]. Moreover, the metal support brings significant enhancements in terms of mechanical and thermal properties for SOFC that opens the way for challenging applications in which such properties are determinant [8]. Among such applications, leveraged by metallic support, are devices to ideally have quick startup and / or require robust mechanical properties, like vehicles.

The decarbonization of transportation comprises an unsolved puzzle set by the simultaneously high gravimetric and volumetric energy density of liquid fuels, which provide easy distribution, sizeable onboard storage, and great autonomy. Thus, a remarkable combination of conversion efficiency, fast recharge, and long-range autonomy can be achieved by using fuel cells fed by a renewable liquid fuel. Among the emerging technologies, direct-ethanol SOFC could immediately reach global markets. Ethanol is the most successful example of biofuel, produced in large scale in different continents with available infrastructure that allows for quick refueling and comfortable handling. Ethanol fueled SOFCs running with good stability have been reported at relative high temperature (~800 °C) in SOFCs with an anodic catalytic layer [9–12]. In such fuel cells the main challenge is to avoid coke formation in the Ni-based composite anode. A successful strategy uses an additional anodic layer active for the ethanol steam reforming reaction that simultaneously prevents the direct contact of the fuel with the Ni cermet and converts ethanol into hydrogen [13–18]. Nonetheless, the active layer must comply with several requirements such as chemical compatibility and high surface area and porosity for not adding mass transport

☆ This article is part of a special issue entitled: 'Solid Oxide Cells' published in Materials Science & Engineering B.

* Corresponding author.
E-mail addresses: fabiocf@usp.br, fcfonseca@ipen.br (F.C. Fonseca).

https://doi.org/10.1016/j.mseb.2025.118259
Received 17 February 2025; Received in revised form 21 March 2025; Accepted 26 March 2025
Available online 29 March 2025

impedance to increase diffusion polarization.

Hydrogen fueled M−SOFC has demonstrated high-performance at significantly reduced operating temperature (~600 °C) with good mechanical properties [19,20]. On the other hand, new challenges are encountered in the realm of M−SOFC. High-chromium ferritic steels are usually the choice for metallic support due to their high corrosion resistance. Thus, careful processing is necessary for the sintering of the cathode and to prevent extensive support oxidation and preserve both the electrical conductivity and the mechanical properties. Therefore, additional thermal treatments to sinter the active layer with tailored microstructure, usually achieved by adding a pore former that requires elimination by oxidation at high temperature, is a complicated task. Moreover, direct ethanol M−SOFC faces an additional challenge because of the poor catalytic properties of the metallic support towards ethanol conversion. As an additional issue, the ethanol steam reforming is facilitated at high temperatures (~800 °C) in which the thermodynamic conditions for carbon deposits are avoided. Therefore, running a direct ethanol M−SOFC in the 600–700 °C range imposes a great challenge for the catalyst performance to ensure long term stability.

In the present study we demonstrate a strategy to add a highly-active catalytic active layer with controlled microstructure by adopting processing parameters compatible with the metal-supported solid oxide fuel cell technology aiming at enhanced stability of direct ethanol M−SOFC running below 800 °C.

2. Experimental

The $La(Cr_{0.8}Ru_{0.2})O_{3-\delta}$ (LCR20) compound was synthesized by the Pechini method, as detailed elsewhere [11,21] for use as catalytic layer in direct ethanol M−SOFC. The material was calcined at 1000 °C for 1 h in air, resulting in single-phase compound. Exsolution of Ru was achieved by a heat treatment of the calcined powder in reducing atmosphere of hydrogen (H_2, 99.999 %) at 900 °C for 4 h [22].

The catalytic properties of the LCR20 were measured at 700 °C during ethanol steam reforming reaction, with a water to ethanol = 3/1 M ratio, in a fixed bed reactor. Details of the experimental protocol for ethanol conversion and product distribution determination are given elsewhere [11,12,22].

Single M−SOFCs by Nissan proprietary technology, with cathode active area of 0.64 cm^2 were kindly supplied by Nissan Japan. This cell is fabricated using 1C44Mo29 (21Cr, Sandvik, Sweden) metal support, anode, and electrolyte all fabricated by tape casting. The 21Cr alloy serves as the metal support, Sc-and-Y-stabilized ZrO_2 (ScYSZ, Daiichi Kigenso, Japan) with pore former is used as the anode, and ScYSZ is used as the electrolyte. Each material is mixed with an organic binder, cast onto Mylar tape, and laminated. A bonding layer consisted of fine 21Cr powder (D50: ~5 μm) mixed with ScYSZ is placed between the metal support and anode electrode to reduce interfacial resistance. The laminate is debinded in air and then sintered at 1250 °C for 1 h in a 10 % H_2/ 90 % Ar atmosphere. After sintering, a 1 μ m GDC layer is deposited on the electrolyte surface via PVD, followed by wet infiltration of a Ni/GDC catalyst onto the anode and initially calcined at 800 °C for 30 min in air. This is followed by two further infiltration and calcination steps, each conducted at 650 °C for 30 min in air. Finally, an LSC (DOWA Holdings, Japan) cathode is applied to the GDC barrier layer by screen printing.

As-received single-cells were tested in H_2/air to ensure achieving the expected electrochemical performance. All fuel cell electrochemical tests were carried out in a Fiaxell SOFC Technologies™ test rig. Typical flow rates of H_2 and synthetic air (80 % N_2 / 20 % O_2) were 200 ml/min for each gas set by mass flow controllers. The electrochemical workstation Zahner IM6 was used to collect I-V data.

The LCR20 catalyst, previously reported [11], was used as the active layer in the M−SOFC for the electrochemical characterization and durability test under ethanol.Prior to the deposition of the catalytic layer, gold was painted on the anode, and a gold wire was fixed to the metallic support surface with gold ink for current collection. In order to meet the M−SOFC constrains imposed by the metallic substrate oxidation, alcohol-based catalyst suspensions were developed. These suspensions eliminate the need for additional heat treatment to remove organic component, thus preventing oxidation of the metallic support. The catalytic ink, based on the LCR20 ceramic powder, was prepared by ball milling the catalytic powder with isopropanol immediately followed by its deposition on the metal support of MS-SOFC by the airbrush technique.

To enhance the catalytic surface area, pore-formers are often incorporated to the active layer. Such pore-formers usually require high temperature treatment in oxidizing atmosphere for their burn out. In this study, an innovative pore former, oxalic acid (20 wt%), was added to the suspension and tested in M−SOFC. The simultaneous thermogravimetric and differential temperature analysis (TG/DTA) of the pore formers was conducted by Setaram LabSys equipment using a heating rate of 10 °C min^{-1} in the 25–1200 °C temperature range under flowing synthetic air (50 ml min^{-1}). The effectiveness of the pore-former was evaluated by examining the microstructure of the catalytic layer deposited on a YSZ substrate using the JEOL JSM-6010LA scanning electron microscope (SEM). Image-J software was used to calculate the pore size and distribution using SEM images of fractured surfaces of the deposited layers with different pore formers.

The electrochemical characterization and the durability tests under ethanol were performed on M−SOFC with catalytic layer (CL-M−SOFC) carried out in the same Fiaxell SOFC Technologies™ test rig using Crofer as the sample holder with Au current collectors in both the air outlet and on the fuel side to avoid any catalytic interference from the measurement setup. A dedicated gas and ethanol/steam delivery system was constructed in house. This system uses mass flow controllers and is connected to a digital interface operated by a personal microcomputer running a home-made software to monitor and accurately control flow rates of all reactants supplied to the fuel cell. Mass flows for synthetic air (cathode), N_2, and H_2 were previously calibrated using a reference Agilent flow meter G6692A. Typical gas flow rates were 200 ml min^{-1} for both the cathode and the total flow mixture to the fuel side. Both ethanol and steam were independently supplied by controlling the temperature of heated gas-tight stainless-steel bottles with a thermocouple and temperature controller by flowing N_2 as a carrier gas. The fuel mixture is delivered to the anode side by a heated pipeline kept at 120 °C to avoid liquid condensation. The electrochemical data, I-V curves, were obtained by the Zahner IM6 workstation. Heating up the cells followed the fabricant protocol and included the cathode in situ sintering as a first step. The fuel cells were initially operated under H_2 and the electrochemical measurements were carried out. Then, fuel cells were polarized (0.6 or 0.7 V) at 700 °C for the durability tests. After typically 10 h of operation, hydrogen was gradually changed to ethanol (or ethanol/water mixture). Two stoichiometric ratios of ethanol to water, 1:1 and 1:2, were used during the durability tests, resulting in gas compositions of 13 % ethanol and 13 % H_2O and 20 % ethanol and 40 % H_2O, carried by N_2 flow.

Post durability test analysis of the samples were performed by Raman spectroscopy experiments of both fragments of the catalytic layer from the surface of the fuel cell and cross sections of the metal support.

3. Results and Discussion

Previous reports from our group demonstrated that a M−SOFC face severe degradation when running on dry ethanol, as the output current density collapses within a few minutes of operation [11]. Such a feature is directly related to the poor catalytic properties of the metal support. Previous fixed bed catalytic tests of ethanol steam reforming revealed that the metallic support leads to poor ethanol conversion and high selectivity to acetaldehyde, which is a carbon deposit precursor [11]. Such results evidence an important limitation imposed to the direct ethanol M−SOFC, which is significantly different from the standard anode support Ni/YSZ that exhibits good activity for ethanol reforming

[11,23]. Thus, to ensure stable operation, direct ethanol M−SOFC needs considerable improvement. The application of an anodic catalytic layer for ethanol reforming in the M−SOFC, utilizing the highly active $LaCr_{0.8}Ru_{0.2}O_3$ (LCR20) catalyst was evaluated. Detailed investigation of the properties of the LCR20 catalyst are reported elsewhere [11,24]. The 20 at.% ruthenium substitution for chrome in $LaCrO_3$ results in single-phase perovskite with minimal structural distortion and remarkable activity for ethanol steam reforming, as compared to the parent compound $LaCrO_3$. The structural features are attributed to the solid solution formation with the comparable ionic radii of the VI-coordinated Cr^{+3} (0.615 Å), Ru^{+4} (0.62 Å), and Ru^{+3} (0.68 Å). The catalytic activity is ascribed to small (~2 nm) ruthenium species that emerge from the solid solution to the surface of the perovskite during the steam reforming reaction [11,24]. The LCR20 compound was found to convert 100 % ethanol to 70 % of H_2 production at 700 °C, as shown in Fig. 1. The catalyst exhibits excellent stability measured for more than 200 h of steam reforming reaction. The main products along with H_2 are 23 % CO and 7 % CO_2. Characterization of spent catalyst revealed no coking in the LCR20 in such conditions [11,24].

Therefore, such an outstanding catalyst, compatible with the SOFC technology, was tested as the catalytic layer in metal-supported SOFC. Fig. 2 shows the current density from a durability test performed on a CL-M−SOFC using 90 mg of the LCR20 catalyst. Initially, the cell was operated with hydrogen for ~ 12 h, maintaining a current density of 1.1 A cm^{-2} at 0.6 V and 700 °C. The fuel was then switched to humid ethanol at a 1:1 ratio, for circa 5 h, when the current density stabilized close to 0.4 A cm^{-2}. Subsequently, the water was removed, and the total operation time was 65 h. In dry ethanol, the current density initially showed a fast decay during the initial 10 h reaching ~ 0.2 A cm^{-2} at ~ 30 h of durability test, after which a much less pronounced degradation was observed. The CL-M−SOFC ran on dry ethanol for ~ 45 h reaching a final current density of ~ 0.15 A cm^{-2} when the test was interrupted after a total 50 h of operation with ethanol.

This initial result shows the significant enhancement of the CL-M−SOFC with a catalytic layer with respect to the standard M−SOFC, which collapsed within few minutes to zero current output when ethanol was used [11].

As the fuel cell showed a relatively fast degradation as compared to the catalytic fixed bed tests, a second test was conducted by increasing the catalyst amount by over 40 %, using a catalytic layer with a total amount of 130 mg of LCR20 deposited onto the anode. Fig. 3 shows the current density as a function of time for this test, where H_2 was initially used as the fuel, stabilizing the current density at 2.7 A cm^{-2} for ~ 10 h. Such a higher current output of these M−SOFC single cells, as compared to the sample in Fig. 2, is attributed to both enhanced current collection and sample-to-sample variability of fabrication processes. When humid ethanol was added at a 1:1 ratio, a significant drop in current density was observed in relation to H_2, reaching ~ 1.2 A cm^{-2}, with a fast decrease to ~ 0.9 A cm^{-2} during the initial 20 h under ethanol. The water/ethanol mixture helped to improve the fuel cell stability; however, the electric current showed a progressive decrease, from ~ 0.9 to 0.3 A cm^{-2}at a practically constant rate over the subsequent 60 h of measurement. After total 100 h of experiment, the fuel cell reached negligible current output and the test was terminated.

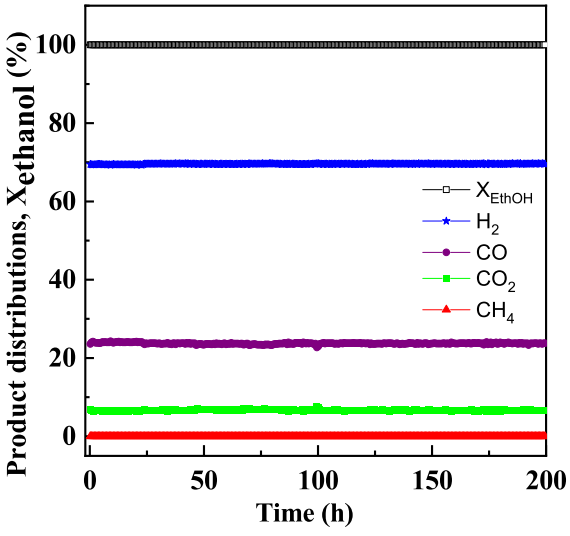

Fig. 1. Ethanol steam reforming using LCR20 catalyst at 700 °C. Ethanol conversion ($X_{ethanol}$) and product distribution [11,24] as a function of time on stream at 700 °C and water/ethanol = 3/1 M mixture.

After adding a larger amont of the catalyst and keeping a 1:1 water to ethanol mixture, the main parameter for further enhancement of the M−SOFC was the microstructure of the catalytic layer. Such a strategy was estimulated by the good catalytic results of the same LCR20 catalyst obtained in ethanol steam reforming reactions in fix bed tests (Fig. 1) [11]. In such tests, in which the ethanol stream flows trough the catalytic powder bed, a complete conversion of ethanol was achieved along with a high (~70 %) and stable production of H_2. As far as the catalytic layer is concerned, the main difference between the two systems is defined by the residence time of the ethanol stream within the catalyst. Thus, the interaction of the inlet fuel with the active material was increased by increasing the porosity of the catalytic layer. Controlling the pore size distribution can enhance the active surface of the catalytic layer. A larger fraction of pores increases the residence time of ethanol in the anode compartment to allow further ESR reaction trough the catalytic layer. Usually, porosity in SOFC functional layers is induced by adding a pore former, such as celulose, starch, or graphite. Pore formers are usually removed by oxidation during the sintering process inhibiting the densification of the functional layer. Thus, pore formers require a high temperature treatment in oxidizing atmosphere to burn out and leave a porous microstructure after sintering. However, the M−SOFC impose some processing constrains that limit high temperature heat treatment in oxidizing environmest to avoid undesired oxidation of the metal support. Thus, a careful selection of pore former was performed to adopt a material that can be eliminated in safe conditions for the M−SOFC. Among some inert materials with low temperature burn out, oxalic acid was tested and selected as an efficient pore former. To determine the apropriate heat treatment required for the removal of this sacrificial agent, termogravimetric analysis (TGA) was conducted. Fig. 4 shows the termogravimetric and differential scanning calorimetry (DSC) curves for 10 mg oxalic acid. These curves show a primary thermal event at 200 °C, corresponding to the complete decomposition of the material.

The effect of the added pore former was investigated in layers deposited onto yttria-stabilized zirconia substrates and fired under the same temperature and N_2 gas flow protocol used for activation of the M−SOFC for the electrochemical characterization. Fig. 5 shows the SEM images of the LCR20 layer without (Fig. 5a) and with oxalic acid (Fig. 5b). It is evident that adding the pore former had the desired effect on the microstructure of the layer, promoting a larger fraction of larger pores than that observed in the LCR20 layer without the oxalic acid. Image analysis of the SEM micrographs in Fig. 5, estimated that sample with oxalic acid addition has an average pore size 0.86 ± 1.02 μm with an average porosity of 43 %, while the sample without pore former exhibits 0.41 ± 0.25 μm average pore size and 26 % porosity. Despite of possible inaccuracy due to the analyses performed in fractured surfaces images, it is evident that oxalic acid considerably increased both the pore size distribution and the total porosity of the deposited layer. Such an increased porosity is likely to enhance the residence time of the ethanol stream in the catalytic layer further promoting the ESR.

Thus, a new suspension containing isopropanol and oxalic acid was used for the deposition of the catalytic layer. Sintering of the layer was caried out in situ similarly to the previous ones, i.e., during the heat up protocol followed for testing the M−SOFC described in the previous section.

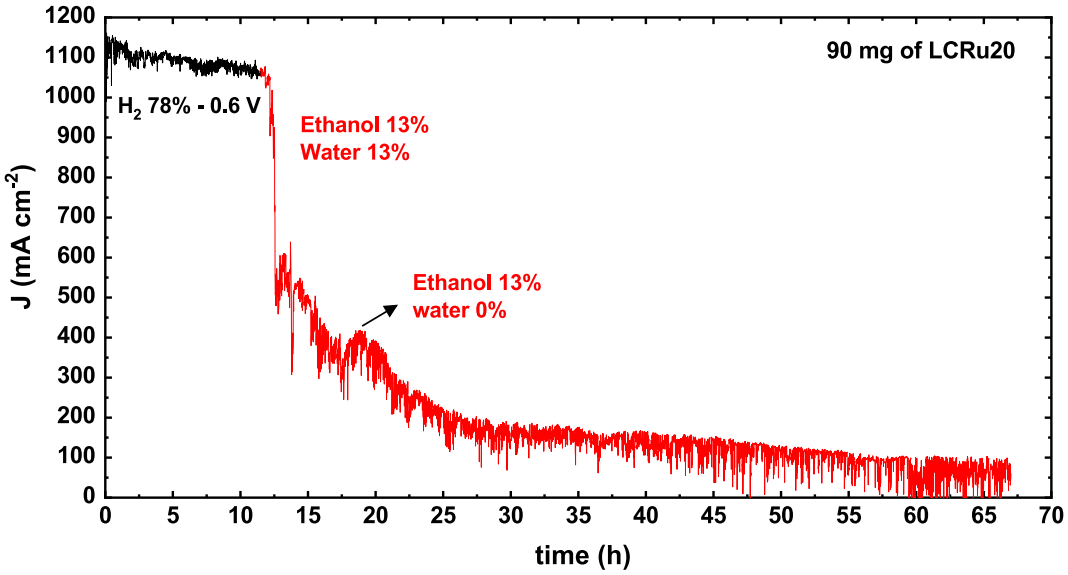

Fig. 2. Durability test of metal supported-SOFC with LCR20 catalytic layer at 700 °C and applied voltage of 0.6 V under H_2 and anhydrous ethanol (13 %). An ethanol / water = 1/1 mixture was used for a during changing from H_2 to dry ethanol.

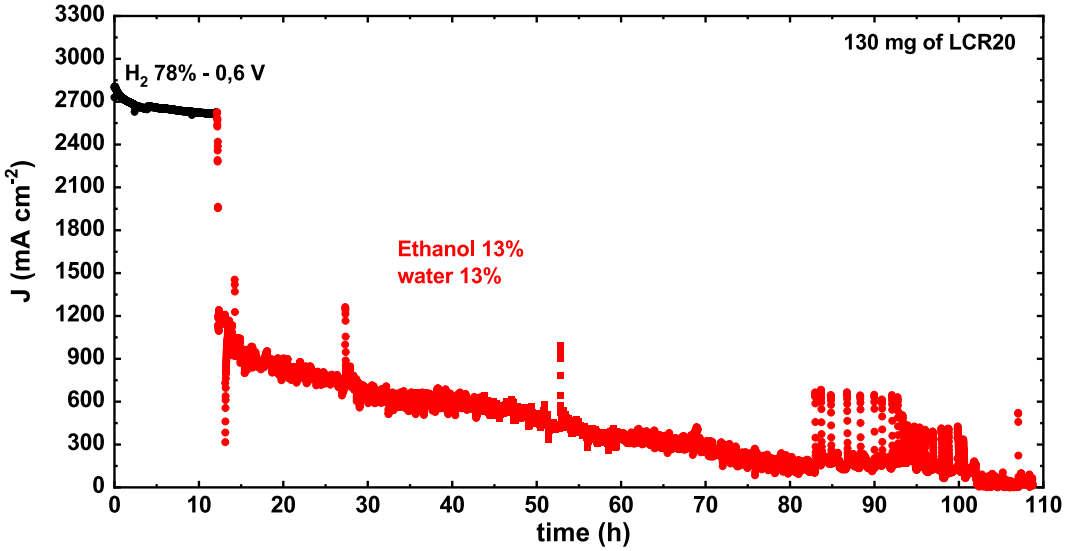

Fig. 3. Durability test of metal supported-SOFC with LCR20 catalytic layer at 700 °C and applied voltage of 0.6 V under H_2 and ethanol/water = 1/1 (ethanol 13 %).

The CL-M−SOFC with enhanced porosity of the LCR catalyst was tested in ethanol, as shown in Fig. 6. In this test, enhanced stability was pursued by ensuring that enough water was provided to the system to avoid carbon deposition. The durability test was conducted using a fuel mixture with a higher water content and ethanol concentration compared to previous tests, and with a reduced applied voltage of 0.7 V. Such parameters aimed aimed at increased fuel utilization. Fuel utilization is proportional to the electrical current drawn from the cell and, consequently, to the steam produced by the electrochemical oxidation of hydrogen. In previous studies of direct (dry) ethanol in anode support SOFC with catalytic layer a fuel utilization factor close to 30 % was estimated for stable operation in dry ethanol [14]. Nevertheless, it is difficult to ensure all possible reaction pathways in such a complex system in which electrochemical, catalytic, and gas-phase reactions may occur. Thus, an additional increase in the water / ethanol ratio = 2 was set to inhibit coking. The fuel cell operated initially on H_2 at 0.7 V for ~ 5 h delivering ~ 1.5 A cm^{-2} The fuel was then switched to ethanol/water and the current dropped to an average 0.7 Acm^{-2} on humid ethanol. The increased volume of steam in the fuel stream caused fluctuations of the measured current values in Fig. 6.

The M−SOFC cell operated in such conditions with relatively good stability for circa 80 h, when a more pronounced degradation continuously reduced the current density to ~ 0.3 A cm^{-2} after 120 h of operation. This result confirms a considerably enhanced stability of the fuel cell and indicates that an active catalytic layer with an optimized microstructure can bring significant improvement for the operation under ethanol.

Despite the enhanced stability, a clear performance degradation was observed. Focusing on possible degradation arising due to the operation under ethanol, post-test analyses aimed at possible observation of carbon deposits. Post durability test analysis of the samples revealed that only in the sample tested without adding water showed a clearly observable carbon deposit. The Raman spectroscopy data (Fig. 7) of fragments of the catalytic layer detected the characteristic bands D and G at 1350 and 1610 cm^{-1}, respectively, associated with carbon only for the sample in Fig. 2 tested with dry ethanol. Samples tested with a

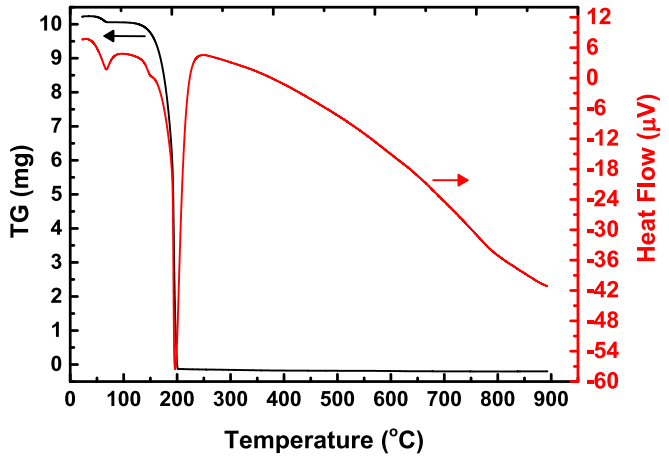

Fig. 4. Simultaneous thermogravimetric and differential temperature analyses of oxalic acid.

mixture of ethanol and steam showed no evidence of carbon formation. Such result is in agreement with the fixed bed reactor catalytic tests of ethanol steam reforming reaction in which no degradation due to carbon deposition was observed for the Ru-LaCrO catalyst. Raman spectroscopy analyses were carried out after durability test on the fractured surfaces of the metal supports. Small peaks of carbon band D at 1320 cm^{-1} in the metallic support indicated amorphous carbon deposits as a possible source of performance degradation of the samples tested with ethanol/water mixtures. As reported in Ref. [24], detailed studies of the LCR catalytic properties were carried out in ESR conditions of partial ethanol conversion ($X_{ethanol} < 100$ %) to evaluate the deactivation mechanism [24]. Such experiments discarded coking or sintering of the active metallic sites. Deactivation of the catalyst was related to the weakly adsorbed species blocking the active ruthenium sites [24]. New experiments are underway to fully uncover the deactivation mechanisms of the LCR catalyst. Concerning the MS-SOFC, carbon formation cannot be excluded and further investigations are necessary to reveal the intricate relations of the operating parameters to ensure stable operation. It is worth mentioning that several degradation mechanisms can take place along with coking, including intrinsic ones related to the metal support

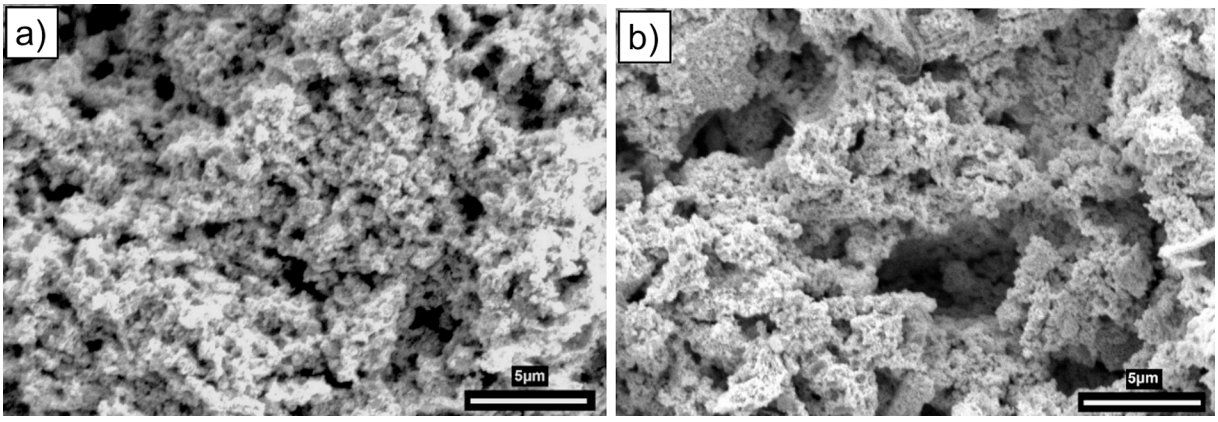

Fig. 5. SEM micrographs of the cross section of deposited LCR20 and sintered layers onto YSZ substrates. Images show the catalyst layer without (a) and with oxalic acid pore former (b).

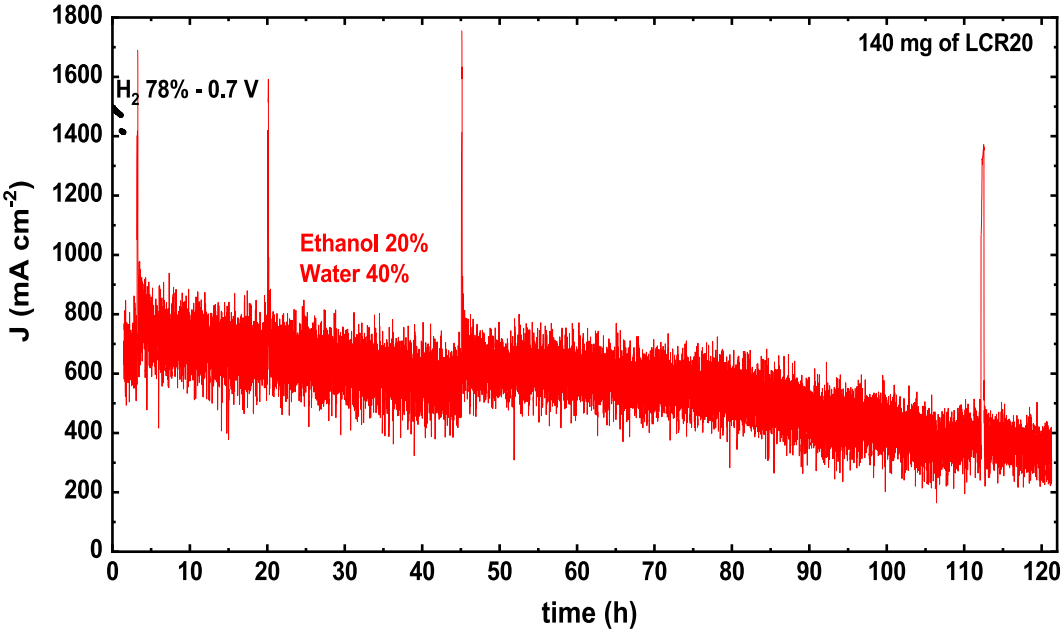

Fig. 6. Durability test of metal supported-SOFC with LCR20 porous catalytic layer at 700 °C and applied voltage of 0.7 V under H_2 andethanol/water = 1/2 (ethanol 20 %).

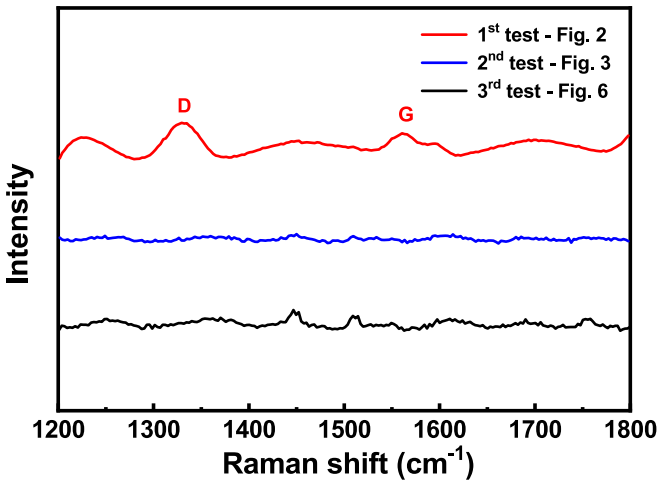

Fig. 7. Raman spectroscopy of the catalytic layer post durability test of metal supported-SOFC. The carbon bands D and G are marked for the sample measured under dry ethanol (Fig. 2).

technology such as support oxidation and clogging. Nonetheless, the experimental results indicate that if enough steam is supplied to an active catalyst significant carbon formation in MS-SOFC is hindered.

4. Conclusion

The metal supported solid oxide fuel cell, with high current output, showed significant progress for the stable operation under ethanol. The strategy included adding a highly active catalytic layer based on the ruthenium derived from solid solution in the $LaCrO_3$ perovskite. Such material exhibits excellent catalytic properties and compatibility with the SOFC components. By adding a catalytic layer onto the metal support resulted in a great enhancement of the performance of the fuel cell running on ethanol without any drawback for the operation under hydrogen. Increasing the thickness of the catalytic layer resulted in enhanced stability. By tailoring the microstructure of the active layer using a suitable pore former to enhance porosity and, thus, the fuel residence time within the catalyst layer, the fuel cell can run on humidified ethanol for more than 100 h. Such a result represents a considerable improvement of the performance of the metal-supported solid oxide fuel cell and points to effective strategies to achieve stable performance in ethanol.

CRediT authorship contribution statement

S.G.M. Carvalho: Writing – review & editing, Writing – original draft. **F.N. Tabuti:** Investigation, Data curation. **E.I. Santiago:** Writing – review & editing, Formal analysis. **R. Abe:** Resources, Project administration, Funding acquisition. **R.M. Guimarães:** Resources, Project administration, Methodology. **Y. Miura:** Methodology, Investigation, Formal analysis. **Y. Fukuyama:** Project administration, Methodology, Investigation, Formal analysis. **F.C. Fonseca:** Conceptualization, Project administration, Funding acquisition, Investigation, Supervision, Writing – review & editing.

Declaration of competing interest

The authors declare that they have no known competing financial interests or personal relationships that could have appeared to influence the work reported in this paper.

Acknowledgments

Authors would like to acknowledge the support from Nissan and the Brazilian agencies CNEN, CNPq Sis-H_2 grant n° 407967/2022-2, and FAPESP grants n° 2023/14931-8 and 2023/10639-0. FCF and EIS are CNPq fellows.

Data availability

Data will be made available on request.

References

[1] E.D. Wachsman, K.T. Lee, Lowering the temperature of solid oxide fuel cells, Science 334 (2011) (1979) 935–939, https://doi.org/10.1126/science.1204090.
[2] B.C.H. Steele, A. Heinzel, Materials for fuel-cell technologies, Nature 414 (2001) 345–352, https://doi.org/10.1038/35104620.
[3] A. Choudhury, H. Chandra, A. Arora, Application of solid oxide fuel cell technology for power generation - A review, Renew. Sustain. Energy Rev. 20 (2013) 430–442, https://doi.org/10.1016/j.rser.2012.11.031.
[4] F. Ramadhani, M.A. Hussain, H. Mokhlis, S. Hajimolana, Optimization strategies for Solid Oxide Fuel Cell (SOFC) application: A literature survey, Renew. Sustain. Energy Rev. 76 (2017) 460–484, https://doi.org/10.1016/j.rser.2017.03.052.
[5] M. Cimenti, J.M. Hill, Direct utilization of liquid fuels in SOFC for portable applications: Challenges for the selection of alternative anodes, Energies (basel) 2 (2009) 377–410, https://doi.org/10.3390/en20200377.
[6] P. Holtappels, H. Mehling, S. Roehlich, S.S. Liebermann, U. Stimming, SOFC system operating strategies for mobile applications, Fuel Cells 5 (2005) 499–508, https://doi.org/10.1002/fuce.200400088.
[7] M.C. Tucker, Progress in metal-supported solid oxide fuel cells: A review, J Power Sources 195 (2010) 4570–4582, https://doi.org/10.1016/j.jpowsour.2010.02.035.
[8] M.C. Tucker, G.Y. Lau, C.P. Jacobson, L.C. DeJonghe, S.J. Visco, Stability and robustness of metal-supported SOFCs, J Power Sources 175 (2008) 447–451, https://doi.org/10.1016/j.jpowsour.2007.09.032.
[9] M. Dewa, J. Han, L. Fang, F. Liu, C. Duan, A.M. Hussain, Y. Miura, S. Dong, Y. Fukuyama, Y. Furuya, N. Dale, O.G. Marin-Flores, S. Saunders, M.G. Norton, S. Ha, NiMo/CZ internal reforming layer for ethanol-fueled metal-supported solid oxide fuel cell, Int J Hydrogen Energy 50 (2024) 1408–1416, https://doi.org/10.1016/j.ijhydene.2023.07.047.
[10] B. Hu, G. Lau, K.X. Lee, S. Belko, P. Singh, M.C. Tucker, Ethanol-fueled metal supported solid oxide fuel cells with a high entropy alloy internal reforming catalyst, J Power Sources 582 (2023) 233544, https://doi.org/10.1016/j.jpowsour.2023.233544.
[11] M. Machado, F. Tabuti, F. Piazzolla, T. Moraes, R. Abe, R.M. Guimarães, Y. Miura, Y. Fukuyama, F.C. Fonseca, Steam Reforming Catalytic Layer on Anode-Supported and Metal-Supported Solid Oxide Fuel Cells for Direct Ethanol Operation, ECS Trans 111 (2023) 301–311, https://doi.org/10.1149/11106.0301ecst.
[12] A.A.A. da Silva, M.C. Steil, F.N. Tabuti, R.C. Rabelo-Neto, F.B. Noronha, L. V. Mattos, F.C. Fonseca, The role of the ceria dopant on Ni / doped-ceria anodic layer cermets for direct ethanol solid oxide fuel cell, Int J Hydrogen Energy 46 (2021) 4309–4328, https://doi.org/10.1016/j.ijhydene.2020.10.155.
[13] N.K. Monteiro, F.B. Noronha, L.O.O. Da Costa, M. Linardi, F.C. Fonseca, A direct ethanol anode for solid oxide fuel cell based on a chromite-manganite with catalytic ruthenium nanoparticles, Int J Hydrogen Energy 37 (2012) 9816–9829, https://doi.org/10.1016/j.ijhydene.2012.03.157.
[14] M.C. Steil, S.D. Nobrega, S. Georges, P. Gelin, S. Uhlenbruck, F.C. Fonseca, Durable direct ethanol anode-supported solid oxide fuel cell, Appl Energy 199 (2017) 180–186, https://doi.org/10.1016/j.apenergy.2017.04.086.
[15] S.D. Nobrega, M.V. Galesco, K. Girona, D.Z. De Florio, M.C. Steil, S. Georges, F. C. Fonseca, Direct ethanol solid oxide fuel cell operating in gradual internal reforming, J Power Sources 213 (2012) 156–159, https://doi.org/10.1016/j.jpowsour.2012.03.104.
[16] P. Frontera, A. Malara, M. Boaro, A. Felli, A. Trovarelli, A. Macario, Ruthenium/nickel ex-solved perovskite catalyst for renewable hydrogen production by autothermal reforming of ethanol, Chem. Eng. Res. Des. 194 (2023) 401–409, https://doi.org/10.1016/j.cherd.2023.04.059.
[17] N.H. Hao, Y. Kim, K. Lee, J. Hwang, J.-S. Park, High performance of direct ethanol-fueled protonic ceramic fuel cells via ethanol steam reforming using non-noble metal catalysts, Electrochim Acta 481 (2024) 143994, https://doi.org/10.1016/j.electacta.2024.143994.
[18] S. Lou, X. Meng, N. Liu, L. Shi, A-site deficient titanate perovskite surface with exsolved nickel nanoparticles for ethanol steam reforming, Chem Eng Sci 274 (2023) 118690, https://doi.org/10.1016/j.ces.2023.118690.
[19] S.R. Hui, D. Yang, Z. Wang, S. Yick, C. Decès-Petit, W. Qu, A. Tuck, R. Maric, D. Ghosh, Metal-supported Solid Oxide Fuel Cell Operated at 400~600oC, ECS Trans 7 (2007) 763–769, https://doi.org/10.1149/1.2729164.
[20] S. (Rob) Hui, D. Yang, Z. Wang, S. Yick, C. Decès-Petit, W. Qu, A. Tuck, R. Maric, D. Ghosh, Metal-supported solid oxide fuel cell operated at 400-600 °C, J Power Sources 167 (2007) 336–339. dOI: 10.1016/j.jpowsour.2007.02.070.
[21] V.B. Tinti, D. Marani, A.S. Ferlauto, F.C. Fonseca, V. Esposito, D.Z. de Florio, Exsolution of Nickel Nanoparticles from Mixed-Valence Metal Oxides: A Quantitative Evaluation by Magnetic Measurements, Part. Part. Syst. Char. 37 (2020), https://doi.org/10.1002/ppsc.201900472.
[22] F. Piazzolla, T.S. Moraes, S.S. Figueiredo, D.F. de Paula, E.L. dos Santos Veiga, C. B. Rodella, F.C. Fonseca, Exsolution of Ni nanoparticles from

La0.4Sr0.4Ti0.8Ni0.2O3-δ perovskite for ethanol steam reforming, Catal Today 444 (2025) 115011, https://doi.org/10.1016/j.cattod.2024.115011.

[23] F.C. Fonseca, F. Tabuti, T. Moraes, R. Abe, R.M. Guimarães, Y. Miura, Y. Fukuyama, Exploring the Stability of Direct Ethanol Solid Oxide Fuel Cells at Intermediate Temperature, ECS Trans 103 (2021) 109.

[24] Tinti B., T.S. Moraes, D.Z. de Florio, A.S. Ferlauto, A. Datye, J. Miller, Y. Miura, F. C. Fonseca, Enhanced ethanol reforming with catalytic active ruthenium species derived from solid solution in lanthanum chromite, ACS Catal submitted, Feb 25 (2025).